INCREASED FLUTTER VELOCITY WITH USE OF A PASSIVE CONTROL SYSTEM

Fabio Itamar de Carvalho*, Roberto Gil Annes da Silva*
***Instituto Tecnológico de Aeronáutica, São José dos Campos, SP, 12228-900, Brazil**

Keywords: *Aeroelastic, Flutter, Coupling, Camber, Velocity, Theodorsen*

Abstract

This paper evaluates a mathematical model of 3 degrees of freedom (DOF), with different coupling factors between flaps (leading and trailing edges), to increase flutter velocity, known as the LAMBIE model [1]. This passive control airfoil concept with mechanical coupling factor between flaps, decreases camber when loading increases and increases camber when loads are smaller. To determine the structural matrices, the Lagrange equation is used and the aerodynamic matrices are determined by the Theodorsen model. This study contemplates simulation results of aeroelastic stability in the frequency domain. The method employed for the calculation of flutter is V-g [4]. In these simulations performed in MATLAB® software, it is possible to increase the velocity at which the flutter phenomenon occurs in 24.41%.

Nomenclature

$\bar{A}$	aerodynamic matrix
B_{NC}	aerodynamic damping matrix
b	mid-chord
$C(k)$	Theodorsen function
CAD	Computer Aided Design
DOF	degrees of freedom
D	dissipation energy
F_{AERO}	aerodynamics forces
d_h	damping heaving motion
d_θ	damping pitching motion
d_γ	damping leading-edge motion
d_β	damping trailing-edge motion
h	linear displacement
I	moment of inertia
ig	damping artificial
K	stiffness matrix
K_C	aerodynamic stiffness matrix
k	reduced frequency
k_h	stiffness degree of freedom q_1
k_θ	stiffness degree of freedom q_2
k_γ	stiffness degree of freedom q_3
L	lift per unit span
L_{gr}	Lagrangian
M	mass matrix
M_{NC}	aerodynamic mass matrix
M_β	trailing-edge moment
M_γ	leading-edge moment
M_θ	pitch moment
n	coupling factor
Q	normal velocity induced ¾ of the chord or b/2 (downwash circulation)
q	generalized coordinates
R	matrix relative to circulatory terms
S_1	displacements coefficients matrix relative to downwash circulation
S_2	velocities coefficients matrix relative to downwash circulation
S	distance from the elastic center to the mass center
T	kinetic energy
U	flow velocity
U_p	potential energy
ω	frequency domain
χ_l	distance from the elastic center of the airfoil to the elastic center of the leading edge
χ_t	distance from the elastic center of the airfoil to the elastic center of the trailing edge

Greek symbols

β	angular displacement of the trailing-edge flap
γ	angular displacement of the leading-

	edge flap
θ	angular displacement (pitch angle)

Subscripts

C	circulatory
D	dynamics
f	main section
ij	array terms indices
l	leading-edge
NC	non-circulatory
t	trailing-edge

1 Introduction

The motivation for this study is to understand the passive systems that could be implemented in aircraft wings to increase the velocity of flutter occurrence. Flutter is a dynamic aeroelastic phenomenon defined as the self-excitation of two or more vibration modes of a system. These modes are modified and feedbacked by fluid flow over the structure. The phenomenon may cause oscillations with amplitudes that grow exponentially, leading the system to structural failure. This instability occurs from the interaction among aerodynamic, inertial and elastic forces, where the fluid flow is excitation energy.

The development of control systems for flutter suppression in aircraft requires complex mathematical models and design techniques. An aeroelastic model of flutter suppression was studied by ZENG et al. [2]. who presented a feedback control based on an experimental model. With such type of control, the flexible dynamics can be consistently estimated via identification system algorithms and its undesirable effects were suppressed through a robust feedback control law, while the stability of the entire system remained.

A very interesting trend in the concept of flutter's suppression phenomenon is the use of acoustic excitations in aerodynamic flow, as in the work of LU and HUANG [3], which presents the theory practiced in this concept.

2 Description of the Aeroelastic Model

The aeroelastic study of this work presents the theoretical basis and numerical methodology for simulation of the 3DOF model, being the movements of the airfoil; bending, pitching and torsion of the coupled flaps. The results of the aeroelastic stability simulations will be calculated in the frequency domain. In order to determine the structural matrices, the Lagrange equation is used and the aerodynamic matrices are determined by Theodorsen model. Coupling factors between the flaps settings 1 to 5 are used, after the simulations it is possible to verify the gain in the flutter velocity. The results of the simulations taking coupling factors 2 to 5 between the flaps are compared with the coupling factor of 1. This passive control airfoil concept using mechanical coupling factor between the flaps, decreases camber when the loading is increased and increases camber when loads decrease. The simulations are performed in Matlab® software. **Fig. 1** illustrates schematically the model of 3DOF.

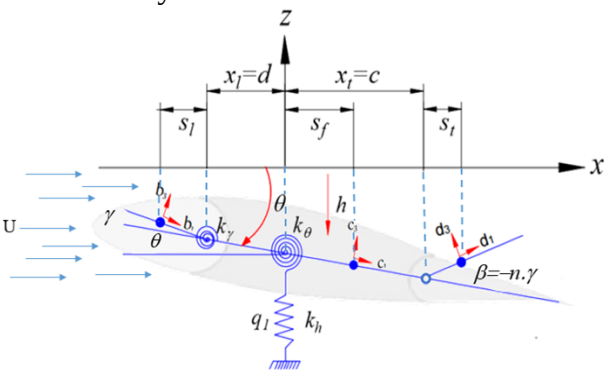

Fig. 1. Aeroelastic Model 3DOF

In the following sections it is presented the methodology used to calculate the structural and aerodynamic models. To ease the understanding, the linearized motion equation is given by:

$$M(\ddot{q}_k) + D(\dot{q}_k) + K(q_k) = F_{aero}(\ddot{q}_k \dot{q}_k, q_k) \quad (1)$$

2.1 Structural Model

The airfoil consists of a wing section with flaps, as presented in **Fig. 1**. The degree of freedom with respect to the wing downward displacement is represented here by *h*. It also describes the translational displacement of the wing elastic line in the airfoil section. The degree of freedom

relative to the wing angular displacement is represented by θ, which represents the angle of inclination of the elastic line in the plane of the airfoil section. The degree of freedom related to the angular displacements of the leading-edge flap is represented by γ and degree of freedom regarding to the angular displacement of the trailing-edge flap, represented by β. The movements of γ and β are in relation to the angle of inclination θ. The flaps movements are mutually dependent on each other. However, the degree of freedom relative to angular displacements of the trailing-edge flap, represented by $\beta = -n\gamma$, is dependent on the angular deflection of the degree of freedom from the leading-edge flap, represented by γ. There is a kinematic coupling factor between the flaps given by n. Thus, the displacements considered for this type of 3DOF and coupled flap airfoil can be represented by a generalized coordinate vector q. The generalized coordinates q_k are:

$$q_{k=}\begin{Bmatrix} q_1 \\ q_2 \\ q_3 \end{Bmatrix} = \begin{Bmatrix} h \\ \theta \\ \gamma \end{Bmatrix} \tag{2}$$

For the calculation of the equations of motion, it is used the Lagrange formalism in function of generalized coordinates (q_k).

$$\frac{d}{dt}\left(\frac{\partial L_{gr}}{\partial \dot{q}_k}\right) - \frac{\partial L_{gr}}{\partial q_k} + \frac{\partial D}{\partial \dot{q}_k} = Q_k \tag{3}$$

The Lagrangian (Lgr) of a system is defined as:

$$L_{gr} = T - U_p + D \tag{4}$$

From kinematics shown in **Fig. 1**, airfoil with 3DOF, coupled flaps, the equation of motion applying Lagrange is given by:

$$\frac{d}{dt}\left(\frac{\partial L_{gr}}{\partial \dot{h}}\right) - \frac{\partial L_{gr}}{\partial h} + \frac{\partial D}{\partial \dot{h}} = m\ddot{h} + S_\theta \ddot{\theta} + S_\gamma \ddot{\gamma} - nS_\beta \ddot{\gamma} + K_h + d_h \dot{h} \tag{5}$$

$$\frac{d}{dt}\left(\frac{\partial L_{gr}}{\partial \dot{\theta}}\right) - \frac{\partial L_{gr}}{\partial \theta} + \frac{\partial D}{\partial \dot{\theta}} = S_\theta \ddot{h} + I_\theta \ddot{\theta} + \left(I_\gamma + S_\gamma (s_l + x_l)\right)\ddot{\gamma} - n\left(I_\beta + S_\beta (s_t + x_t)\right)\ddot{\gamma} + K_\theta + d_\theta \dot{\theta} \tag{6}$$

$$\frac{d}{dt}\left(\frac{\partial L_{gr}}{\partial \dot{\gamma}}\right) - \frac{\partial L_{gr}}{\partial \gamma} + \frac{\partial D}{\partial \dot{\gamma}} = S_\gamma \ddot{h} - nS_\beta \ddot{h} + \left(I_\gamma + S_\gamma (s_l + x_l)\right)\ddot{\theta} - n\left(I_\beta + S_\beta (s_t + x_t + s_l + x_l)\right)\ddot{\gamma} + K_\gamma \gamma + d_\gamma \dot{\gamma} + n^2 d_\beta \dot{\gamma} \tag{7}$$

2.2 Aerodynamic Model

This subsection presents the aerodynamic loads acting on the airfoil with 3DOF: lift force in h direction and aerodynamic moments in relation to angles θ, γ and $\beta\,(-n\gamma)$. **Fig. 1** illustrates the schematic drawing used for aerodynamic loading calculations on the 3DOF airfoil. The functions of Theodorsen, T and Z [9] are used for non-stationary aerodynamic modeling. Theodorsen's function is deficiency lift function that modifies the circulation over the airfoil by induced normal velocity. The reduced frequency is the argument k of the Theodorsen function $C(k)$ [4]. The normal velocity induced ¾ of the chord or $b/2$, Q (downwash). Thus, considering the coupling factor between the flaps of $n=-\beta/\gamma$ for the numerical model of 3DOF, is given as:

$$Q = U\theta + \dot{h} + b\dot{\theta}\left(\frac{1}{2} - a\right) + \frac{Z_{13}}{\pi} U\gamma + \frac{Z_{11}}{2\pi} b\dot{\gamma} - n\frac{T_{10}}{\pi} U\gamma - n\frac{T_{11}}{2\pi} b\dot{\gamma} \tag{8}$$

The generalized coordinates q_k are defined for each degrees of freedom shown in equation (2). Thus, considering a simple harmonic motion (MHS), the 3DOF reads:

$$h = \bar{h}e^{i\omega t} \tag{9}$$

$$\theta = \bar{\theta}e^{i\omega t} \tag{10}$$

$$\gamma = \bar{\gamma}e^{i\omega t} \tag{11}$$

Definitions of the aerodynamic forces acting with movement between the coupled flaps:

$$F_{Aero} = \begin{Bmatrix} -L \\ M_\theta \\ M_\gamma + nM_\beta \end{Bmatrix} \tag{12}$$

Equation of the lift in the direction h and aerodynamic moments in relation to the angles θ and γ:

$$\begin{aligned} L = & -\pi\rho b^2 \left(U\dot{\theta} + \ddot{h} - ba\ddot{\theta} - \frac{Z_1}{\pi} U\dot{\gamma} \right. \\ & \left. + \frac{Z_2}{\pi} b\ddot{\gamma} + n\frac{T_4}{\pi} U\dot{\gamma} + n\frac{T_1}{\pi} b\ddot{\gamma} \right) \\ & -2\pi\rho UbQC(k) \end{aligned} \tag{13}$$

$$\begin{aligned} M_\theta = & -\pi\rho b^2 \left[\left(\frac{1}{2} - a\right) Ub\dot{\theta} \right. \\ & + b^2 \left(\frac{1}{8} + a^2\right) \ddot{\theta} - ba\ddot{h} + \frac{Z_{16}}{\pi} U^2\gamma \\ & + \frac{Z_{17}}{\pi} Ub\dot{\gamma} + \frac{Z_4}{\pi} b^2\ddot{\gamma} - n\frac{T_{15}}{\pi} U^2\gamma \\ & \left. - n\frac{T_{16}}{\pi} Ub\dot{\gamma} - n\frac{2T_{13}}{\pi} b^2\ddot{\gamma} \right] \\ & + 2\pi\rho Ub^2 C(k) Q \left(a + \frac{1}{2}\right) \end{aligned} \tag{14}$$

$$\begin{aligned} M_\gamma = & -\rho b^2 \left[Z_{20} Ub\dot{\theta} + Z_4 b^2\ddot{\theta} + Z_2 b\ddot{h} \right. \\ & - \frac{Z_{23}}{\pi} U^2\gamma - \frac{Z_{24}}{2\pi} Ub\dot{\gamma} + \frac{Z_8}{\pi} b^2\ddot{\gamma} \\ & + n\frac{Z_{21}}{\pi} U^2\gamma - n\frac{Z_{22}}{2\pi} Ub\dot{\gamma} \\ & \left. - n\frac{Z_{12}}{\pi} b^2\ddot{\gamma} \right] + \rho Ub^2 QZ_{15} C(k) \end{aligned} \tag{15}$$

The aerodynamic moments, $M\gamma + M_\beta$, with relation to the angle γ, using the coupling factors n between the flaps:

$$\begin{aligned} M_\beta = & \rho b^2 \left[nT_{17} Ub\dot{\theta} + n2T_{13} b^2\ddot{\theta} \right. \\ & - nT_1 b\ddot{h} - n\frac{Z_{18}}{\pi} U^2\gamma - n\frac{Z_{19}}{\pi} Ub\dot{\gamma} \\ & + n\frac{Z_{12}}{\pi} b^2\ddot{\gamma} - n^2\frac{T_{18}}{\pi} U^2\gamma \\ & \left. + n^2\frac{T_{19}}{2\pi} Ub\dot{\gamma} + n^2\frac{T_3}{\pi} b^2\ddot{\gamma} \right] \\ & + n\rho Ub^2 QT_{12} C(k) \end{aligned} \tag{16}$$

Assuming harmonic motions of the airfoil, taking into account the boundary conditions adopted, it is necessary that work performed reads:

$$\dot{W} = -\left[L\dot{h} + M_\theta\dot{\theta} + \left(M_\gamma + nM_\beta\right)\dot{\gamma} \right] \tag{17}$$

2.3 Numerical Methodology

The method used is V-g, also known as "k" method, which is a technique used to calculate aeroelastic stability, divergence and flutter. Note the system to be solved is an eigenvalue problem [4]:

$$\frac{1 + ig}{\Omega^2} \left[\bar{K}_{ij}\right]\{\bar{q}_k\} = \left[\bar{A}_{ij} + \bar{M}_{ij}\right]\{\bar{q}_k\} \tag{18}$$

The V-g method assumes there is an artificial damping g, indicating the damping required for simple harmonic motion.
Dividing the equations of motion by mass and nondimensionalizing by b, the equations read:

$$\frac{1+ig}{-\omega^2}[\bar{K}]\{\bar{q}_k\} = [\bar{M}]\{\bar{q}_k\} + \frac{1}{\mu}\left(\frac{1}{k^2}C(k)\{R\}[S_1]\{\bar{q}_k\} - i\frac{1}{k}C(k)\{R\}[S_2]\{\bar{q}_k\} - [M_{NC}]\{\bar{q}_k\} + i\frac{1}{k}[B_{NC}]\{\bar{q}_k\} + \frac{1}{k^2}[K_C]\{\bar{q}_k\}\right) \quad (19)$$

Structural and aerodynamic matrices can be defined by the equations of the sections 2.1 and 2.2 [10]. Table 1 shows the properties used to calculate flutter speed.

Tab. 1. Airfoil Properties

Description	Value	Units (SI)
m_f	22	kg
m_l	12	kg
m_t	10	kg
S_f	0.10	m
S_l	0.05	m
S_t	0.07	m
x_l	0.10	m
x_t	0.40	m
I_f	0.56	kgm
I_l	0.12	kgm
I_t	0.10	kgm
k_h	2500	N/m
k_θ	2962.7	Nm/rad
k_γ	3600	Nm/rad
$2b$	1	m

In these calculations of flutter, the energy dissipation function D are not employed. The artificial damping g, which indicates the damping required for simple harmonic motion (MHS), is used instead. Only in the condition of flutter, this artificial damping has physical meaning, i.e., when g=0.

4 Results

For the aeroelastic calculations, it is necessary to define the characteristics and properties of the airfoil. The results are presented considering 5 coupling factors between flaps at leading and trailing edges. The coupling coefficients in simulations are n=1, n=2, n=3, n=4 and n=5. Figures 2 to 6 present the results of artificial damping and frequency (Hz) in function of the flow velocity.

In **Fig. 2**, considering the coupling factor between the flaps being n=1, flutter occurs at the velocity of 196.45 m/s and the frequency of 11.51 Hz in the torsion mode of the airfoil. Note the curve related to the damping factor associated with the degree of freedom γ(torsion between the flaps) is not very sensitive to the capability to extract or dissipate energy from the flow to coupling factor n=1.

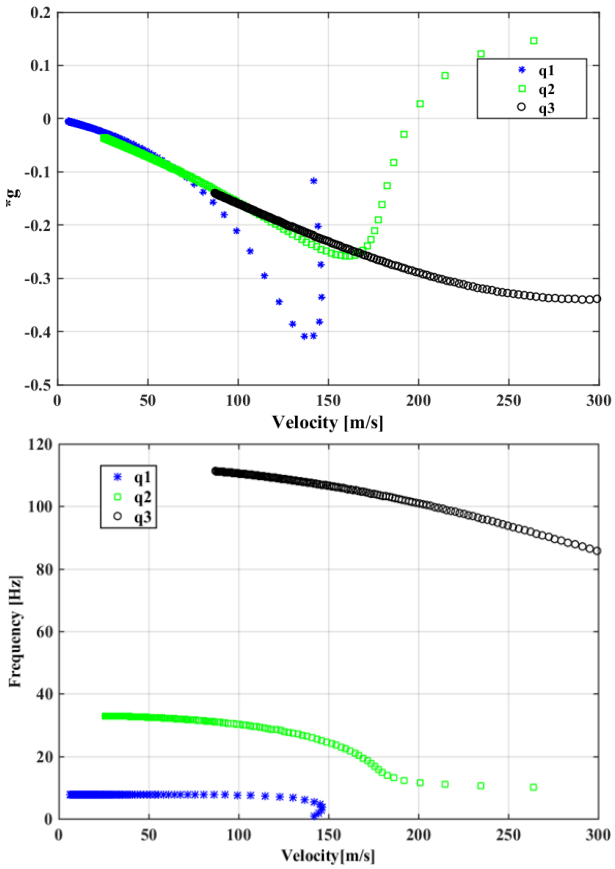

Fig. 2. Coupling Factor *n*=1

In **Fig. 3**, considering the coupling factor between the flaps being n=2, flutter occurs at the highest velocity, 226.3 m/s and the frequency of 11.53 Hz, associated with the torsion mode of the

airfoil. Note the frequencies of the torsion mode of the flaps decreased with the increase of the coupling factor for n=2. The mode representing the coupling between the flaps has been shown to be more efficient in the capability to extract and dissipate energy from the flow, which is also observable from the evolution of frequencies with velocities, when compared to the case of n=1.

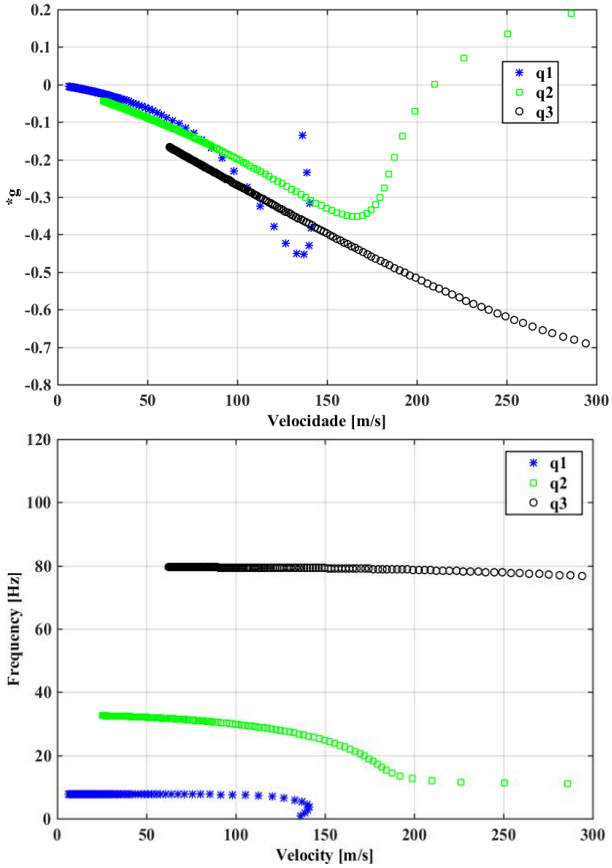

Fig. 3. Coupling Factor n=2

Fig. 4 to **Fig. 6** show the results with larger coupling factors between the flaps n=3, n=4 and n=5. In these cases, the increase of the coupling factor implies an increase in the effective camber between the flaps. Since the transmission ratio or coupling factor create an incremental linear dependence, on the magnitude of the flap displacement amplitude of the trailing edge when the leading-edge flap deflects. As can be seen in the presented results in the following section, the higher is the increase of the coupling factor, the larger is the amount of energy from the flow that flaps are able to extract. Also, the coupled modes will tend to combine with the twisting mode of the wing section, which implies in the increase of flutter velocity. So, what is effectively observed is the ability of coupling between the bending and pure torsion modes of the section to be degraded with the tendency to promote coupling between the pure and coupled torsion modes between the flaps, as the transmission ratio increases.

It can be seen from the results presented that flutter occurs at velocity of 236.0 m/s and frequency of 12.02 Hz, which is the torsion mode of the airfoil for the coupling factor of n=3 between the flaps. With coupling factor n=4, the flutter velocity occurs at 241.5 m/s and frequency of the torsion mode in 12.3 Hz. For coupling factor n=5, the flutter velocity occurs at 243.7 m/s and frequency of 12.41 Hz. These flutters velocities increase in function of the coupling factors.

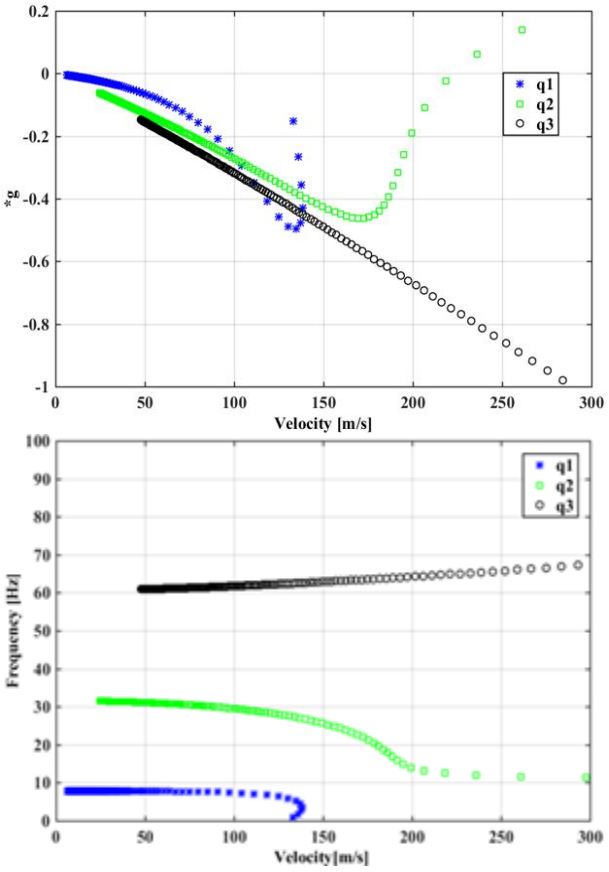

Fig. 4. Coupling Factor n=3

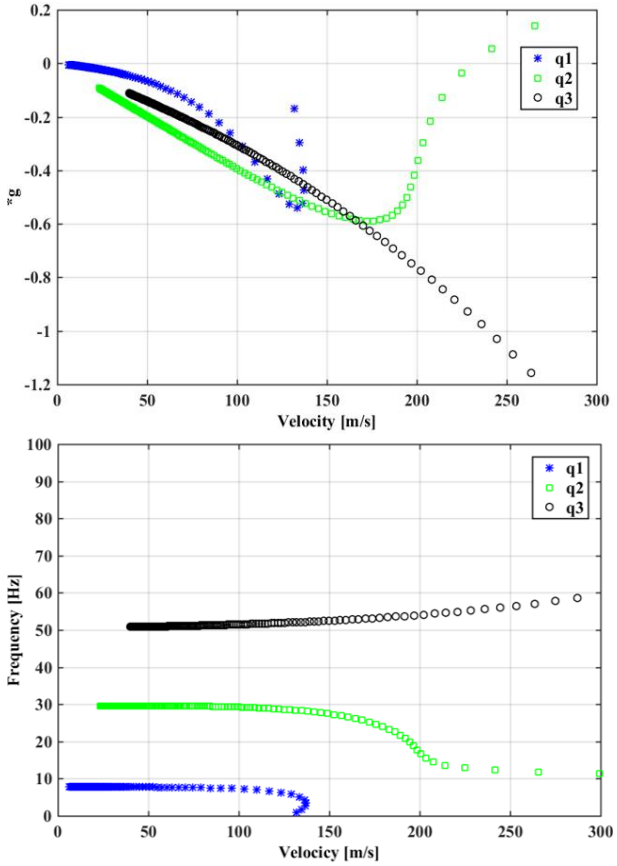

Fig. 5. Coupling Factor n=4

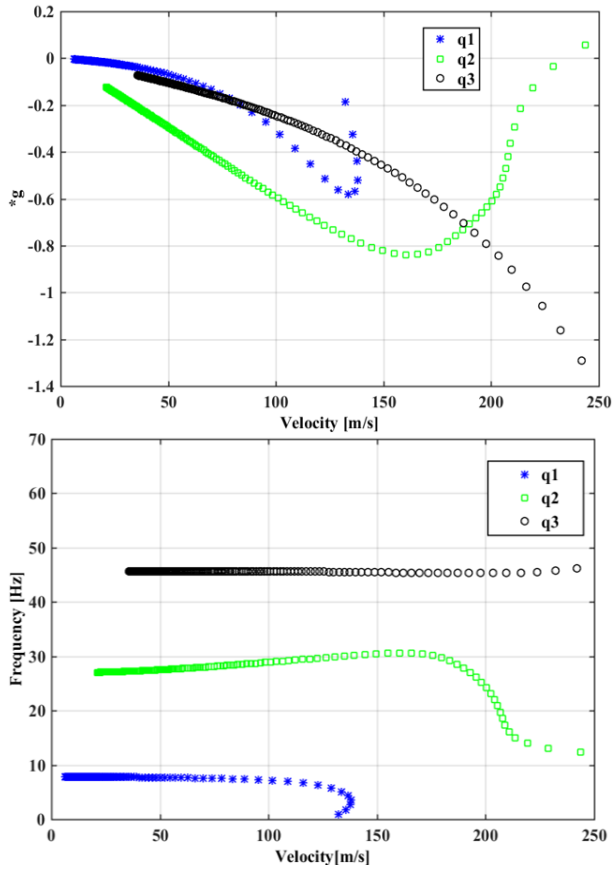

Fig. 6. Coupling Factor *n*=5

Table 2 presents the velocity and frequency summary of the aeroelastic stability simulations shown in the previous Figures, in which the flutter occurs according to the coupling factor.

Tab. 2. Comparison of the Flutter Velocity

Coupling Factor	Velocity Flutter (m/s)	Frequency Flutter (Hz)
1	196.45	11.51
2	226.30	11.53
3	236.00	12.02
4	241.50	12.03
5	243.70	12.41

5 Conclusion

In this study an increase of the velocity in which the flutter occurs is obtained in 24,41% using the coupling mode n=5, when compared with the velocity obtained with n=1. Using the actuation of the flaps coupled through a mechanism coupling. By increasing the coupling factors, the flutter velocity also increases. In the calculations performed, the flutter velocities for the coupling factors n=1 and n=5 are respectively 196.45 m/s and 243.7 m/s. It was observed the model presents ability of coupling between bending mode and pure torsion mode of the section are degraded. This fact, happens because of the tendency to promote coupling between the pure torsion mode and coupled torsion mode between the flaps, increasing the coupling ratio.

These simulations of aeroelastic stability of the numerical model with 3DOF verify that coupling factors of 2 and 3 are sufficient to modify the mechanism of energy extraction of the modes of the aeroelastic system. Thus, migrating from the standard flexo-torsional coupling to the torsional of the section and between the flaps. It can also be seen in Table 2 that coupling factors above 3 do not occur a high gain of flutter suppression.

The associated energies of each degree of freedom q_1, q_2 and q_3, bending movements, pure torsion of the section and torsion of flaps become more and more sensitive, according to the increase of the coupling factor. Thus, the

velocities at which the flutter phenomenon occurs increases with the coupling factor.
By this concept of coupling mechanism between the flaps and camber changes, the flight velocities can be increased by 24,41%. Also, this concept can be used in aircraft designs which requires to fly in high velocities.

6 Future Work

Future work to complement the current could explore the following subjects:

- Design of a device for experimental testing of a wing in scale with 3DOF.
- Evaluation of the test results in comparison with the numerical model used for the aeroelastic stability calculations.
- Evaluation of flap lengths and mass balance, since in the current simulations performed it is verified that model has a great sensitivity to the position of center of mass.
- Analysis of fatigue life of the coupled flaps, due to the number of oscillations, aiming to application of the concept in aircraft wings, unmanned aerial vehicles (UAVs) or even in rotating wings.
- Addition of the energy dissipation function in the calculations and check damping and gain rates on flutter suppression.
- Introduction of flexible wings by different types of materials.

References

[1] Lambie B. *Aeroelastic Investigation of a Wind Turbine Airfoil with Self-Adaptive Camber*. 2011. 159 p. Thesis (PhD in Fluid Mechanics and Aerodynamics (SLA) – Department of Mechanical Engineering) - Technischen Universitat Darmstadt, Darmstadt.

[2] Zeng J, Kukreja L. S and Moulin B. Experimental Model-Based Aeroelastic Control for Flutter Suppression and Gust- Load Alleviation. *Journal of Guidance, Control and Dynamics*, Vol. 35, No. 5, pp 1377-1390, 2012.

[3] Lu P and Huang L. Optimal Control Law Synthesis for Flutter Suppression Using Active Acoustic Excitations. *Journal of Guidance Control and Dynamics*, Vol. 16, No.1, pp 124-131, 1993.

[4] Bisplinghoff H. L, Ashley H and Halfman R. L. *Aeroelasticity*. Reading MA, Addison-Wesley, 1955.

[5] Wright J. R. and Cooper J. E. *Introduction to Aircraft Aeroelasticity and Loads*. 2nd ed. New York, John Wiley, 2015.

[6] Spiegelberg H. *Adaptive Camber Airfoil for Load Alleviation in Horizontal Axis Wind Turbines: Analytical and Numerical Study*. 2015. 165 p. Thesis (PhD in Dynamics and Vibrations – Department of Numerical Methods in Mechanical Engineering) - Technischen Universitat Darmstadt, Darmstadt.

[7] Lambie B, Krenik A and Tropea C. Numerical Simulation of an Airfoil with a Flexible Trailing Edge in Unsteady Flow. In: *AIAA/ASME/ASCE/AHS/ASC STRUCTURES, STRUCTURAL DYNAMICS AND MATERIALS CONFERENCE*, 51., 2010, Orlando, FL. Proceedings… Reston: AIAA, 2010.

[8] Lambie B, Jain M, Tropea C and Spelsberg-Korspeter, G. Passive Camber Change for Windturbine Load Alleviation. In: *AIAA-2011-637 AEROSPACE SCIENCES MEETING INCLUDING THE NEW HORIZONS FORUM AND AEROSPACE EXPOSITION*, 49. 2011, Orlando, FL. Proceedings… Reston: AIAA, 2011.

[9] Jaworski J. W. Thrust and Aerodynamic Forces from an Oscillating Leading Edge Flap. *AIAA Journal*, Vol. 50, No. 12, pp 2928-2931, Dec. 2012.

[10] Theodorsen T. *General Theory of Aerodynamic Instability and the Mechanism of Flutter*. Washington, DC: NACA, 1935. NACA-TR-496.

7 Contact Author Email Address

mailto: fabcarval@gmail.com
mailto: gil@ita.br

Copyright Statement

The authors confirm that they, and/or their company or organization, hold copyright on all of the original material included in this paper. The authors also confirm that they have obtained permission, from the copyright holder of any third-party material included in this paper, to publish it as part of their paper. The authors confirm that they give permission, or have obtained permission from the copyright holder of this paper, for the publication and distribution of this paper as part of the ICAS proceedings or as individual off-prints from the proceedings.